

## Rotational and Vibrational Excitations of a Hydrogen Molecule Trapped within a Nanocavity of Tunable Dimension

Shaowei Li (李绍巍),<sup>1</sup> Arthur Yu,<sup>1</sup> Freddy Toledo,<sup>1</sup> Zhumin Han (韩竹敏),<sup>1</sup> Hui Wang,<sup>1,\*</sup> H. Y. He,<sup>1</sup> Ruqian Wu,<sup>1</sup> and W. Ho<sup>1,2,†</sup>

<sup>1</sup>*Department of Physics and Astronomy, University of California, Irvine, California 92697-4575, USA*

<sup>2</sup>*Department of Chemistry, University of California, Irvine, California 92697-4575, USA*

(Received 10 July 2013; published 2 October 2013)

The rotational and vibrational transitions of a hydrogen molecule weakly adsorbed on the Au(110) surface at 10 K were detected by inelastic electron tunneling spectroscopy with a scanning tunneling microscope. The energies of the  $j = 0$  to  $j = 2$  rotational transition for para- $\text{H}_2$  and HD indicate that the molecule behaves as a three-dimensional rigid rotor trapped within the tunnel junction. An increase in the bond length of  $\text{H}_2$  was precisely measured from the downshift in the rotational energy as the tip-substrate distance decreases.

DOI: [10.1103/PhysRevLett.111.146102](https://doi.org/10.1103/PhysRevLett.111.146102)

PACS numbers: 68.37.Ef, 33.20.Sn, 63.22.-m, 73.40.Gk

Rotational and vibrational transitions can reveal structural and energetic properties of molecules [1,2]. Even small changes in the distance between atoms or the masses from isotopic substitution alter the rotational and vibrational transition energies of the molecule. The power of vibrational and rotational spectroscopies has been demonstrated in the frequency [3–5] and time [6,7] domains in the infrared and microwave. The sensitivity of vibrational spectroscopy has reached the single bond level by the detection of the vibrationally inelastic electron tunneling process using the scanning tunneling microscope (STM) [8]. However, the detection of rotational transitions in single molecules remains to be demonstrated.

Hydrogen, the lightest element in the universe, plays a particularly important role in the development of quantum mechanics. Exact solutions to the Schrödinger equation can be obtained for atomic and molecular hydrogen. The rotational states of the hydrogen molecule can be analyzed within the rigid rotor model. The smallest mass of hydrogen (H) and the large percent difference in mass from its isotope deuterium (D) yield high and large shifts in energies for the rotational transitions that facilitate detection.

The detection of the rotational transitions of molecular hydrogen using the STM requires that the bonding between molecule and substrate should be sufficiently weak so the adsorbed molecule behaves like a gas phase molecule, but the molecule needs to be sufficiently stable for  $I$ - $V$ ,  $dI/dV$ , and  $d^2I/dV^2$  scanning tunneling spectroscopy (STS). On noble metal surfaces such as Au(110), molecular hydrogen is weakly adsorbed at low temperature via van der Waals (vdW) forces [9,10]. The adsorbed molecules are mobile and can rapidly migrate one by one in and out of the tip-surface tunnel junction, on a time scale much shorter than the imaging time [10,11]. In the tunneling range, the tip-substrate separation is 6.5 to 7.5 Å in our measurement. At the same time, tunneling occurs just below the tip apex, and the tunneling current is confined laterally within the

sub-angstrom range. In such a junction, only a single hydrogen molecule can be trapped at any given time [12,13]. Although the spectroscopic signals are the average over many molecules from the diffusion and trapping processes, each trapped hydrogen molecule is experiencing the same environmental coupling given by the tip-substrate junction, and variations in the configurations and properties of different molecules are expected to be insignificant. The trapped hydrogen molecule dramatically increases the contrast of the STM topographic images, providing new details of complex surface structures [11,12]. In addition, as each trapped molecule is separated from other surrounding molecules, it maintains the essential properties as an isolated molecule that exhibits the rotational and vibrational properties of a nearly free molecule trapped within a nanocavity of tunable dimension.

Here, we demonstrate rotational spectroscopy with the STM. In the inelastic electron tunneling spectroscopy (IETS) with the STM, excitations are characterized as step changes in the  $dI/dV$  spectrum at the threshold voltage corresponding to these excitations. The STM inelastic electron tunneling spectroscopy of  $\text{H}_2$ ,  $\text{D}_2$ , and HD molecules weakly adsorbed on the Au(110) surface shows a series of step changes in the  $dI/dV$  spectra, which correspond to rotational and vibrational excitations. In these  $dI/dV$  spectra,  $j = 0 \rightarrow 2$  rotational excitations of  $\text{H}_2$  and HD are recorded as an increase in conductance while the  $\nu = 0 \rightarrow 1$  vibrational excitations in the adsorption well of  $\text{H}_2$ ,  $\text{D}_2$ , and HD show a decrease in conductance. The coupling of the rotational motions of the hydrogen molecule to its environment given by the metallic tip and substrate is determined by squeezing the tip-substrate separation.

The experiments were performed using a home-built STM operating at 10 K and a base pressure of  $3 \times 10^{-11}$  Torr [14]. The Au(110) surface was cleaned by cycles of  $\text{Ne}^+$  sputtering and annealing at 680 K. The silver tip was electrochemically etched. The clean surface

at 10 K was dosed either with  $\text{H}_2$ , HD, or  $\text{D}_2$  at  $1 \times 10^{-10}$  Torr for 5 min. The adsorb molecule can be completely desorbed by laser illumination at 10 K or raising the sample temperature to 27 K, allowing repeated measurements without the need for tip and sample preparations.

The diffusion and trapping of a molecule in the tunnel junction is illustrated in Fig. 1(a). The topographic STM image [Fig. 1(b)] taken on a hydrogen-free Au(110) surface shows a clear  $2 \times 1$  reconstruction structure. After dosing  $\text{H}_2$ ,  $\text{D}_2$ , or HD, the high resolution image in Fig. 1(c) reveals single Au atoms on atop sites; the Au atoms in the troughs remain unresolved. The  $dI/dV$  image [Fig. 1(d)] and the  $d^2I/dV^2$  image [Fig. 1(e)] also reveal atomic resolution for atop sites. The increased spatial resolution obtained after dosing  $\text{H}_2$ ,  $\text{D}_2$ , or HD indicates that a single hydrogen molecule can be trapped between the tip and an atop Au atom. In this Letter, all the STS spectra were recorded above atop Au atoms.

The rotational motion of adsorbed molecules can either be free or hindered, depending on the depth of the adsorption well. Previous STM studies have investigated the rotational motion of molecules stably adsorbed on the surface and can be imaged [15–17]. In these studies, the molecules are highly constrained to be within the adsorption well and the rotations are described as hindered vibrational modes. However, if the adsorption

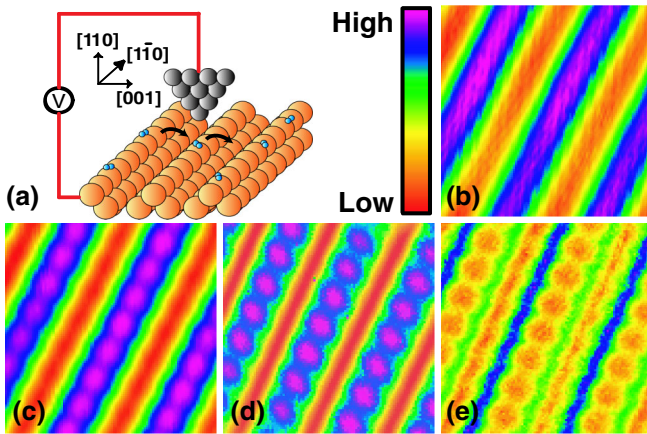


FIG. 1 (color online). (a) Schematic diagram of the diffusion and trapping of a hydrogen molecule in the tunnel junction. The average lifetime of each trapped molecule in the junction is estimated to be far shorter than the response time of STM electronics. The spectroscopic signals arise from the average of many such diffusion and trapping processes. (b) STM topographic image of a bare Au(110)  $2 \times 1$  reconstructed surface obtained at constant current mode prior to dosing with hydrogen. Imaging conditions: tunneling gap set with sample bias  $V_B = 13.5$  mV and tunneling current  $I_T = 2$  nA. (c) STM topographic image obtained under the same conditions as (b) but after dosing with  $\text{H}_2$  molecules. (d)  $dI/dV$  image at 0 mV bias and (e)  $d^2I/dV^2$  image at 10 mV bias for surface adsorbed with  $\text{H}_2$ . Tunneling gap setting conditions:  $V_B = 50$  mV and  $I_T = 2$  nA for (d),  $V_B = 100$  mV and  $I_T = 10$  nA for (e).

potential well is shallow, the rotational motion of the molecule is “unhindered” [18] and is characteristic of a rigid three-dimensional (3D) free rotor. The rotational energy is given by  $j(j+1)\hbar^2/2\mu r_b^2$ , where  $j = 0, 1, 2, \dots$ ,  $\mu$  is the reduced mass of the molecule, and  $r_b$  is the distance between the two atoms in the molecule (the bond length for  $\text{H}_2$ ). In the STS spectra taken on  $\text{H}_2$ , a step change in the  $dI/dV$  spectrum is observed [Fig. 2(a)], with a corresponding peak in the  $d^2I/dV^2$  spectrum [Fig. 2(b)] at 42.0 mV. This energy agrees with the  $j = 0 \rightarrow 2$  rotational excitation of a para  $\text{H}_2$  as a 3D rigid rotor, indicating that the  $\text{H}_2$  molecules on Au(110) behave like they do in the gaseous phase. For the HD, this inelastic rotational signal shifts down to 31.5 mV, which is 0.75 times the measured transition energy of  $\text{H}_2$ , in agreement with the value of  $3/4$  according to the 3D rigid rotor model. Since the two atoms in HD are distinguishable, the  $j = 0 \rightarrow 1$  excitation is allowed. However, this excitation is difficult

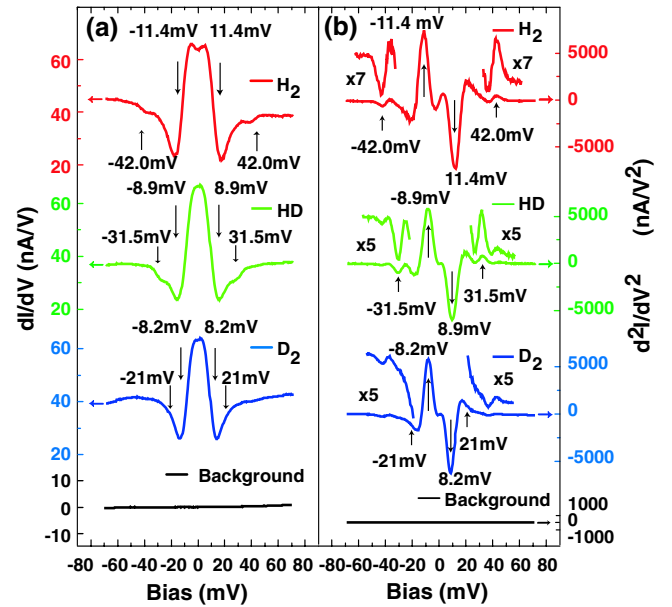


FIG. 2 (color online). Tunneling spectra taken before and after dosing molecular hydrogen or its isotopes. The tunneling gap is set with  $V_B = 50$  mV and  $I_T = 2$  nA for all the spectra. The bias for the  $x$  axis in the spectra has been shifted up by 1 mV to compensate for instrumental offset. (a) From the top to the bottom:  $dI/dV$  spectra of  $\text{H}_2$ , HD,  $\text{D}_2$ , and a clean gold surface (background). (b) From the top to bottom:  $d^2I/dV^2$  spectra of  $\text{H}_2$ , HD,  $\text{D}_2$ , and a clean gold surface (background). The magnified line shapes for the rotational excitation are also presented. The excitation energies are marked by arrows. The signal at  $\pm 42.0$  mV in  $\text{H}_2$  spectra and the signal at  $\pm 31.5$  mV in HD spectra are assigned to the  $j = 0 \rightarrow 2$  rotational excitation. The small structure around  $\pm 42$  mV in the HD and  $\text{D}_2$  spectra is attributed to contamination from co-adsorption of the background  $\text{H}_2$  in the vacuum chamber. The strong signals at  $\pm 11.4$ ,  $\pm 8.9$ , and  $\pm 8.2$  mV in the spectra for  $\text{H}_2$ , HD, and  $\text{D}_2$  are assigned to the  $\nu = 0 \rightarrow 1$  vibrational excitation within the physisorption potential well.

to resolve since its energy is expected to be at 10.5 mV, where the signal is dominated by the  $\nu = 0 \rightarrow 1$  vibrational transition. For the same reason, the  $j = 0 \rightarrow 2$  excitation energy of ortho- $D_2$  at 21 mV is similarly difficult to resolve. On the other hand, the  $j = 1 \rightarrow 3$  rotational excitation at 70 mV for ortho- $H_2$  and 35 mV for para- $D_2$  is not visible in the STS spectra. These results are in agreement with prior measurements by electron energy loss spectroscopy (EELS), showing that hydrogen molecules are weakly adsorbed on noble metal surfaces at low temperature and rapidly convert into the  $j = 0$  state (the para- $H_2$  or ortho- $D_2$ ) [9,16,19]. Thus the presence of ortho- $H_2$  or para- $D_2$  is unlikely on Au(110) at 10 K. Nevertheless, our data for  $H_2$  and HD are sufficient to indicate that molecular hydrogen on Au(110) behaves as a 3D rigid rotor.

The strong signals at lower energies in the tunneling spectra are assigned to the vibrational excitations in the physisorption potential well. In the harmonic approximation, the vibration energies are given by  $h\nu_0(\nu + 1/2)$  with  $\nu = 0, 1, 2, \dots$ . In the tunneling spectra of  $H_2$ , the large step down at 11.4 mV in the  $dI/dV$  spectrum [Fig. 2(a)] and the corresponding asymmetric dip in the  $d^2I/dV^2$  spectrum [Fig. 2(b)] are assigned to the  $\nu = 0 \rightarrow 1$  excitation of the hydrogen vibrational motion bouncing between the tip and substrate. In the tunneling spectra of HD and  $D_2$ , the  $\nu = 0 \rightarrow 1$  transition energy is shifted down to 8.9 and 8.2 mV, respectively. The ratios of these transition energies are 1.3 between  $H_2$  and HD and 1.4 between  $H_2$  and  $D_2$ , in agreement with the quantum harmonic oscillator.

The rotational energy is directly related to the principal moment of inertia of the molecule and, therefore, to its structure [20]. Rotational spectroscopy with the STM can be used to probe changes in the structure of a single molecule due to its coupling to the environment. The rotational excitation energies in Fig. 2 are slightly smaller than the theoretical result for a free molecule (42.0 vs 43.9 mV for  $H_2$  and 31.5 vs 33.1 mV for HD) or the experimental data measured for an ensemble of molecules by electron energy loss spectroscopy (44 mV for  $H_2$  [9,21]). These deviations are presumably caused by changes in the molecular structure due to coupling of the molecule to the tip. The effect of this coupling can be systematically investigated by varying the tip-substrate separation which is controlled by setting the sample bias and tunneling current. As the sample bias decreases from 120 to 5 mV while keeping the tunneling current constant at 2 nA, the tip is moved toward the surface by approximately 1 Å (the tip-substrate separation changes from 7.5 to 6.5 Å). Both the vibrational and rotational excitation energies change during this process. The  $\nu = 0 \rightarrow 1$  vibrational excitation energy of  $H_2$  increases from 7.5 to 18 mV [Fig. 3(d)]. The tunneling spectra for HD show a similar trend when the tip-substrate separation is changed [Fig. 3(b)]. The increase of vibration energy suggests a strengthened bonding of the molecule to the substrate,

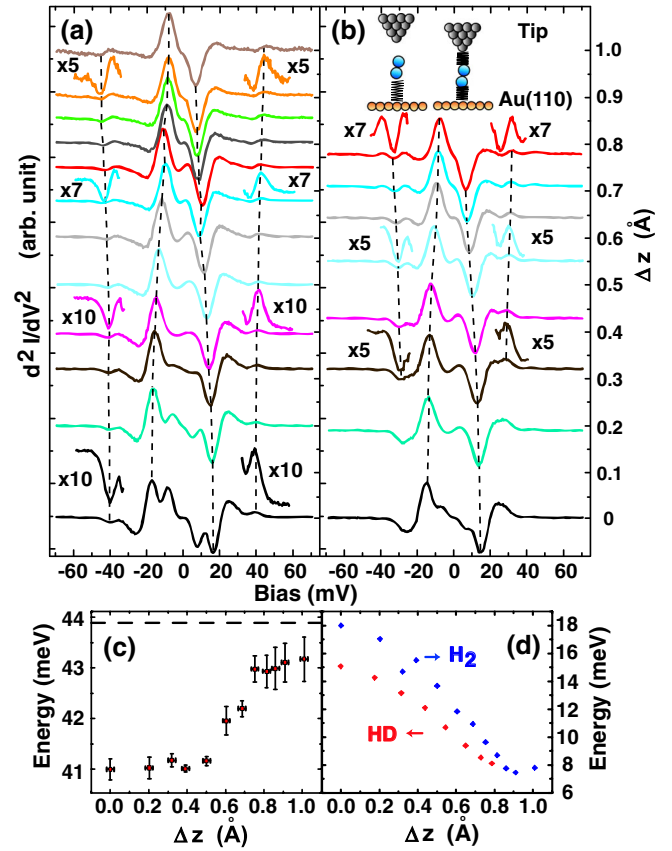


FIG. 3 (color online). (a),(b)  $d^2I/dV^2$  spectra taken at different tip-substrate separation for  $H_2$  (a) and HD (b). The sample bias  $V_B$  is changed from 5 (bottom) to 120 mV (top) in (a) and from 5 (bottom) to 70 mV in (b).  $I_T$  is kept at 2 nA for all these spectra. A  $z$ - $V$  curve is measured to convert the change in  $V_B$  to the corresponding change in the tip-substrate separation ( $\Delta z$ ). The tunneling gap distance at  $V_B = 5$  mV and  $I_T = 2$  nA is used as the reference point ( $\Delta z = 0$ ). The uncertainty in  $\Delta z$  is around 0.095 Å. The shiftings of the rotational and vibrational excitation energies are indicated by the dashed lines. The magnified line shapes of the rotational excitation are also presented. (c) The  $j = 0 \rightarrow 2$  excitation energy of hydrogen increases from 41 to 43 mV as  $\Delta z$  increases by 1 Å. The horizontal dashed line indicates for reference the excitation energy of a free molecule. (d) The  $\nu = 0 \rightarrow 1$  excitation energy decreases from 18 to 7.5 mV as  $\Delta z$  increases by 1 Å for  $H_2$ , and from 15 to 8 mV as  $\Delta z$  increases by 0.8 Å for HD.

which weakens the H-H bond and increases the bond length as predicted by theoretical calculations [22,23]. DFT calculations of the adsorption energy and H-H bond length at different tip-substrate separations have been performed [Fig. 4(a)] using the Vienna *ab initio* simulation package (VASP) at the level of vdW-DF2. An interaction-energy curve of the Morse potential type is revealed, which further confirms that van der Waals interactions are important in this weakly bonding system. According to the calculation, the H-H bond length increases from 0.750 to 0.765 Å when the tip-substrate separation decreases from 7.5 to 6.5 Å. In agreement with the DFT calculations, the rotational

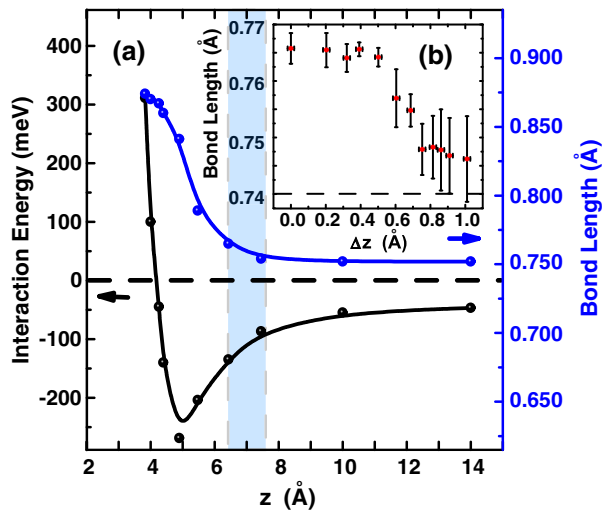


FIG. 4 (color online). (a) DFT calculations of the interaction energy between the trapped molecule and the tunneling junction, and H-H bond length at different tip-substrate separation. The blue shaded area indicates the approximate range probed by STM. (b) The H-H bond length, derived from the measured  $j = 0 \rightarrow 2$  excitation energies, decreases from 0.766 to 0.746 Å as  $\Delta z$  increases by 1 Å. The dashed line indicates for reference the H-H bond length of a free molecule.

excitation energy of  $H_2$  decreases from 43 to 41 mV [Fig. 3(c)] as the tip-substrate separation decreases by  $\sim 1$  Å, indicating that the H-H bond length increases from 0.746 to 0.766 Å [Fig. 4(b)]. DFT calculations also identified the observed vibrational mode as the bouncing motion of  $H_2$  confined between the Au(110) surface and the tip [24].

In summary, the STM has been extended to the study of the rotational excitations of weakly adsorbed molecules, in addition to the detection of vibrational transitions. Rotational spectroscopy at the single molecule level opens a new avenue for chemical identification and measurement of the bond length in a single bond. By squeezing a trapped hydrogen molecule in the tip-substrate junction by decreasing the dimension of the nanocavity, structural changes in a single molecule can be observed by altering the potential experienced by the molecule.

This work is supported by the Chemical Science, Geo- and Bioscience Division, Office of Science, U.S. Department of Energy, under Grant No. DE-FG02-04ER15595. The experimental and theoretical collaboration is supported by the NSF Center for Chemical Innovation on Chemistry at the Space-Time Limit (CaSTL) under Grant No. CHE-0802913.

\*Present address: Department of Physics, Fudan University, Shanghai, China.

†To whom correspondence should be addressed.

wilsonho@uci.edu

- [1] R. C. Jaklevic and J. Lambe, *Phys. Rev. Lett.* **17**, 1139 (1966).
- [2] E. B. Wilson, Jr., *Science* **162**, 59 (1968).
- [3] P. O. Stoutland, R. B. Dyer, and W. H. Woodruff, *Science* **257**, 1913 (1992).
- [4] R. S. McDonald, *Anal. Chem.* **58**, 1906 (1986).
- [5] P. R. Griffiths, *Science* **222**, 297 (1983).
- [6] K. K. Kohli, G. Davies, N. Q. Vinh, D. West, S. K. Estreicher, T. Gregorkiewicz, I. Izeddin, and K. M. Itoh, *Phys. Rev. Lett.* **96**, 225503 (2006).
- [7] C. Schröter, K. Kosma, and T. Schultz, *Science* **333**, 1011 (2011).
- [8] B. C. Stipe, M. A. Rezaei, and W. Ho, *Science* **280**, 1732 (1998).
- [9] K. Svensson and S. Andersson, *Surf. Sci.* **392**, L40 (1997).
- [10] J. A. Gupta, C. P. Lutz, A. J. Heinrich, and D. M. Eigler, *Phys. Rev. B* **71**, 115416 (2005).
- [11] J. R. Hahn and W. Ho, *Phys. Rev. Lett.* **87**, 196102 (2001).
- [12] C. Weiss, C. Wagner, C. Kleimann, M. Rohlfing, F. S. Tautz, and R. Temirov, *Phys. Rev. Lett.* **105**, 086103 (2010).
- [13] W. H. A. Thijssen, D. Djukic, A. F. Otte, R. H. Bremmer, and J. M. van Ruitenbeek, *Phys. Rev. Lett.* **97**, 226806 (2006).
- [14] B. C. Stipe, M. A. Rezaei, and W. Ho, *Rev. Sci. Instrum.* **70**, 137 (1999).
- [15] B. C. Stipe, M. A. Rezaei, and W. Ho, *Science* **279**, 1907 (1998).
- [16] L. J. Lauhon and W. Ho, *J. Chem. Phys.* **111**, 5633 (1999).
- [17] J. K. Gimzewski, C. Joachim, R. R. Schlittler, V. Langlais, H. Tang, and I. Johansson, *Science* **281**, 531 (1998).
- [18] I. F. Silvera, *Rev. Mod. Phys.* **52**, 393 (1980).
- [19] P. Avouris, D. Schmeisser, and J. E. Demuth, *Phys. Rev. Lett.* **48**, 199 (1982).
- [20] B. C. Dian, G. G. Brown, K. O. Douglass, F. S. Rees, J. E. Johns, P. Nair, R. D. Suenram, and B. H. Pate, *Proc. Natl. Acad. Sci. U.S.A.* **105**, 12 696 (2008).
- [21] K. Svensson and S. Andersson, *Phys. Rev. Lett.* **78**, 2016 (1997).
- [22] S. Sakong and A. Groß, *Surf. Sci.* **525**, 107 (2003).
- [23] A. Groß, *Appl. Phys. A* **67**, 627 (1998).
- [24] See Supplemental Material at <http://link.aps.org/supplemental/10.1103/PhysRevLett.111.146102> for more details of the DFT calculations.